HORTSCIENCE 57(8):877–888. 2022. https://doi.org/10.21273/HORTSCI16567-22

Rain-shelter Cultivation Affects the Accumulation of Volatiles in 'Shuijing' Grape Berries during Development

Qingyang Sun, Yue Zhao, Shusheng Zhu, and Fei Du
College of Plant Protection, Yunnan Agricultural University, Kunming, 650201, China

Ruzhi Mao, Lijing Liu, and Yifan Zhu
College of Food Science and Technology, Yunnan Agricultural University, Kunming, 650201, China; and University Engineering Research Center for Grape & Wine of Yunan Province, Yunnan Agricultural University, Kunming, 650201, China

Su Li
College of Horticulture and Landscape, Yunnan Agricultural University, Kunming, 650201, China

Meng Sun
Institute of Pomology, Jiangsu Academy of Agricultural Sciences, Nanjing, 210014, China

Bin Tian
Faculty of Agriculture and Life Sciences, Lincoln University, Lincoln, 7647, New Zealand

Additional index words. open-field cultivation, principal component analysis, table grape, vintage, *Vitis*

Abstract. **Rain-shelter cultivation could protect grape berries from many diseases and affect grape berry quality. However, there have been few studies of the effects of rain-shelter cultivation on the accumulation of volatiles in Shuijing grapes grown in Yunnan Province. Therefore, the goal of this research was to explore the effects of rain-shelter cultivation on the accumulation of volatiles in Shuijing grape berries during development. The Shuijing grapes used during this study were grown in the Yunnan Province of southwest China in two consecutive vintages (2018 and 2019). The results showed that rain-shelter cultivation promoted grape ripening and inhibited volatiles synthesis in Shuijing grape berries. However, the application of rain shelters did not affect the accumulation patterns of volatiles; instead, it affected the concentrations of volatiles in Shuijing grape berries, especially during the maturation phase [12–15 weeks after flowering (WAF)]. The concentrations of isoprenoid-derived volatiles (2019), fatty acid-derived volatiles, and amino acid-derived benzenoids in Shuijing grape berries were decreased by rain-shelter cultivation during the maturation phase. The concentration of 2,5-dimethyl-4-methoxy-3(2H)-furanone (mesifurane) was also decreased by rain-shelter cultivation during the late maturation phase (14 and 15 WAF). A principal component analysis (PCA) indicated that the vintage had a much greater influence on the physicochemical parameters and volatiles of the Shuijing grape berries than the cultivation method. This work reveals the formation and accumulation patterns of volatiles of Shuijing grape berries under rain-shelter cultivation during development and has significance for exploring the potential of rain-shelter cultivation in grape-producing regions with excessive rainfall.**

The Shuijing grape cultivar is one of the traditional table grape cultivars in Yunnan Province and is famous for its unique aroma characteristics. Li et al. (2017) reported that Shuijing could be the local name for Niagara (*V. labrusca* L.) because they have the same genotype and similar morphological characteristics. In Yunnan Province, the maturation of Shuijing grape cultivar coincides with the rainy season, and excessive rainfall could cause outbreaks and epidemics of severe diseases, such as downy mildew, ripe rot, white rot, black rot, brown spot, and grey mold (Du et al., 2015). Widespread disease breakout usually leads to heavy economic loss. To alleviate the losses caused by most diseases induced by excessive rainfall, methods involving cultural practices, resistant cultivars, and fungicides are usually used. Among these methods, rain-shelter (RS) cultivation is a simple, effective, safe, and ecological way to control diseases (Du et al., 2015; Li et al., 2014; Meng et al., 2013; Shi et al., 2018). The rain shelter consisted of a transparent plastic film roof type of structure without sidewalls. This structure could prevent rainfall damage and decrease grape disease incidences. Our previous study found that the average severities of grape ripe rot, white rot, and downy mildew for the Red Globe grape cultivar under RS cultivation were reduced by 93%, 89%, and 94%, respectively, compared with the control (Du et al., 2015). In addition, Chavarria et al. (2007) reported that the plastic overhead cover (similar to RS treatment) decreased the incidence and severity of ripe rot (−76.55% and −89.47%) and grey mold (−39.39% and −57.56%) for Moscato Giallo grape cultivar during the ripening period. Therefore, this technique has been applied to viticulture in rainy regions, especially in Yunnan Province (Du et al., 2015).

In addition to preventing grapevine diseases, many studies have indicated that RS cultivation could affect the quality of grape berries. Compared with grape berries grown under open-field (OF) cultivation, 'Red Globe' grape berries grown under RS cultivation exhibited a higher content of sugar and a lower content of total acid (Du et al., 2015). For Cabernet Gernischet and Cabernet Sauvignon grape cultivars, the contents of most anthocyanin compounds in grape skins were significantly reduced under RS cultivation because of increases in ambient temperature and humidity and decreases in photosynthetically active radiation (*PAR*) (Meng et al., 2013; Shi et al., 2018). Gao et al. (2016) reported that the berry size and the concentration of secondary metabolites (polyphenolic and volatile compounds) were altered by the microclimate variations under rain shelters. It was also reported that RS cultivation affects the accumulation of volatiles in grapes via regulation of biosynthetic gene expression (Bureau et al., 2010; Koyama and Goto-Yamamoto, 2008).

Volatile compounds are important characteristics of grape quality. They are usually located in grape pulp and skin in free and bound glycoside forms (Lund and Bohlmann, 2006). The flavor of table grapes is mainly determined by the free forms of volatiles because they can be sensed and tasted directly compared with the bound glycoside forms (Wu et al., 2016). These volatiles are generally derived from isoprenes, fatty acids, and amino acids via various synthetic pathways (Liu et al., 2015). According to these synthetic pathways, these volatiles can be categorized into terpenoids, norisoprenoids, straight-chain aliphatics, branched-chain aliphatics, benzenoids, and others (Gao et al., 2016). Terpenoids and norisoprenoids are synthesized from common C5 isoprene precursors via the

Received for publication 1 Mar. 2022. Accepted for publication 27 Apr. 2022.
Published online 6 July 2022.
This work was supported by the Major Science and Technology Project in Yunnan Province of China (202001BB050001), the Scientific Research Fund Project of Yunnan Education Department (2020J0243), and the Free Exploration Project for Academicians of Yunnan Science and Technology Department (2018HA009).
Y. Zhu is the corresponding author. E-mail: yifanzhuyy@163.com.

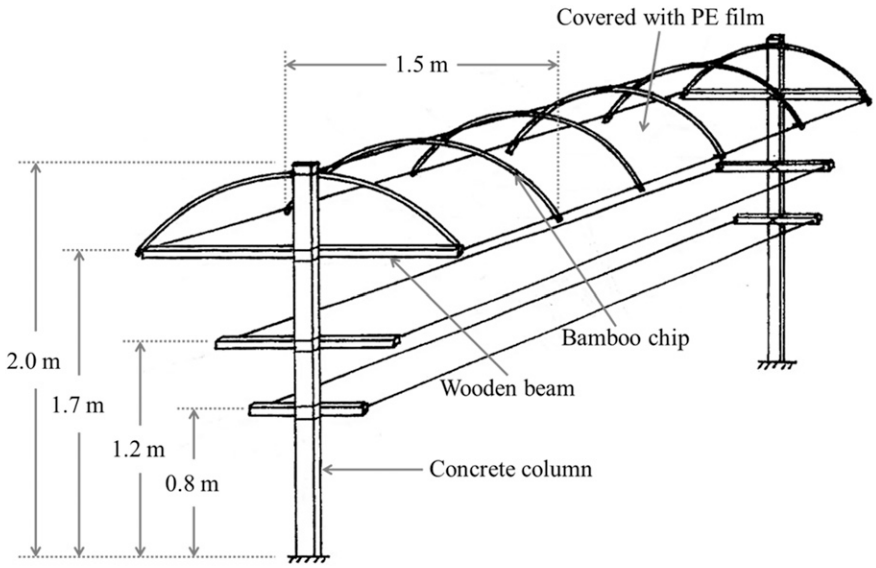

Fig. 1. Schematic illustration of rain shelter and related parameters.

methyl-erythritol-phosphate (MEP) pathway (Gao et al., 2016). The straight-chain aliphatics are represented by C6/C9 compounds and their derivatives, and other straight-chain aliphatics. C6/C9 compounds and their derivatives, including C6 and C9 aldehydes, alcohols, esters, and ketones, are primarily generated through the lipoxygenase–hydroperoxide lyase (LOX-HPL) pathway (Wang et al., 2019). The other straight-chain aliphatics are mainly formed through β-oxidation (Wu et al., 2020) and affected by the activity and specificity of β-oxidation enzymes in the fatty acid metabolism pathway (Dudareva et al., 2004). Branched-chain amino acids (valine, isoleucine, and leucine) are precursors of branched-chain aliphatics, and benzenoids are synthesized from phenylalanine (Dunlevy et al., 2010). The composition and concentration of these volatiles may vary greatly among different cultivars (Noguerol-Pato et al., 2012), cultivation techniques, and environmental factors (Gómez-Míguez et al., 2007).

To our knowledge, the effects of RS cultivation on the accumulation of volatiles in Shuijing grapes grown in Yunnan Province have not been sufficiently investigated. Accordingly, the volatiles in Shuijing grape berries grown under RS cultivation were studied and compared with those in Shuijing grape berries grown under OF cultivation. The results of this study provide a comprehensive understanding of the effects of RS cultivation on the accumulation patterns of volatiles in Shuijing grape berries and could be helpful for estimating the potential of RS cultivation in grape-producing regions with excessive rainfall.

Materials and Methods

Plant material and treatments

This study was conducted in a commercial Shuijing grape vineyard (lat. 24°6′4.84″N, long. 104°3′36.4″E, 1441 m above sea level) in Qiubei County of Yunnan Province (China) during the grape-growing seasons of two consecutive vintages (2018 and 2019). The vines were planted in rows oriented east-to-west and spaced 1.0 m (between vines) × 2.0 m (between rows); they were bilateral cordon-trained and spur-pruned on a standard Y-type trellis. According to the historical meteorological data of the Qiubei County, the mean annual temperature was between 13.2 and 19.7 °C, and the mean annual rainfall level was between 1000 and 1270 mm.

Six rows of vines were selected in the experimental field and divided into two groups by the midpoint. The vines located at the east side of the midpoint were selected for RS cultivation (group 1). The shelter was built along the vine rows at the 5 WAF and removed after harvest (15 WAF). The rainy season of this region starts in May, but the majority of this rainfall occurs between June and August each year. Therefore, the shelter was built in May (≈5 WAF). The rain shelter was 2.0 m high, 1.5 m wide, and covered with a commonly used polyethylene (PE) film (0.08 mm thickness, 85% visible light transmittance, 30% ultraviolet radiation-blocking rate) (Fig. 1). The vines located at the west side of the midpoint were selected for OF (control) cultivation (group 2). For both cultivation methods, three independent, nonadjacent areas were divided to create three experimental replicates (≈50 vines for each replicate), and all experimental vines were managed with the same production management practices.

The Shuijing grape berries were sampled from 4 to 15 WAF (the first rapid growth phase: from bloom to 8 WAF; the veraison (lag) phase: ≈9 –11 WAF; the berry maturation phase: 12–15 WAF) in 2018 and 2019. For each replicate, ≈500 healthy berries were randomly collected on each sampling date from 8:00 AM to 10:00 AM. Afterward, the samples were placed in ice boxes at 4 °C and transported to the laboratory of Kunming within 3 h. Approximately 400 fresh berries of each replicate were used for the determination of physicochemical parameters. The remaining ≈100 berries were immediately frozen in liquid nitrogen, stored at −80 °C, and subsequently used for the determination of volatiles.

Meteorological data (sunshine duration, rainfall, and temperature) were collected by a meteorological weather station located near the experimental site and obtained from the meteorological bureau of Qiubei County. Heat accumulation values were calculated as the growing degree day (GDD_{10}) from bloom until harvest. The GDD_{10} units were calculated using the daily maximum and minimum temperatures with a minimum threshold of 10 °C. The data are shown in Table 1.

Determination of physicochemical parameters

The volume per 100 berries was measured by the displacement method with a measuring cylinder. In addition, ≈100 berries were juiced by an electric juicer, and the resulting juice was centrifuged at 10,000 g_n for 10 min

Table 1. The meteorological data of Shuijing grape-growing season in 2018 and 2019.

	2018				2019			
	Bloom–8 WAF	9–11 WAF	12–15 WAF	Bloom–15 WAF	Bloom–8 WAF	9–11 WAF	12–15 WAF	Bloom–15 WAF
Sunshine duration/h	427.1	78.1	137.5	642.7	427.7	132.9	76.4	637.0
Rainfall/mm	194.6	150.4	139.0	484.0	278.7	64.1	174.8	517.6
Average daily temperature/°C	20.1	20.8	22.8	20.9	21.6	24.1	22.7	22.4
Average daily temperature difference/°C	10.7	8.1	8.1	9.5	12.0	9.8	7.3	10.4
GDD_{10}	699.3	245.5	383.3	1328.1	810.1	312.9	379.3	1502.3
Daily maximum temperature/°C	31.7	29.7	30.6	31.7	34.7	33.0	31.1	34.7
Daily minimum temperature/°C	7.0	14.6	18.5	7.0	7.7	14.0	17.6	7.7

GDD_{10} = growing degree day; WAF = weeks after flowering.

at 4 °C. The juice was analyzed to determine levels of total soluble solids (TSS) using a refractometer (Master-M, Tokyo, Japan) and total acidity by titration with 0.05 N NaOH, followed by pH analysis.

Determination of volatiles

Volatiles from the Shuijing grape berries were extracted by the headspace solid phase microextraction method. The frozen grape berries (100 g) of each replicate and polyvinylpolypyrrolidone (1 g) were ground into powder in liquid nitrogen, macerated at 4 °C for 2 h, and centrifuged to obtain Shuijing grape juice. The juice (5 mL) was transferred to a 15-mL airtight vial with

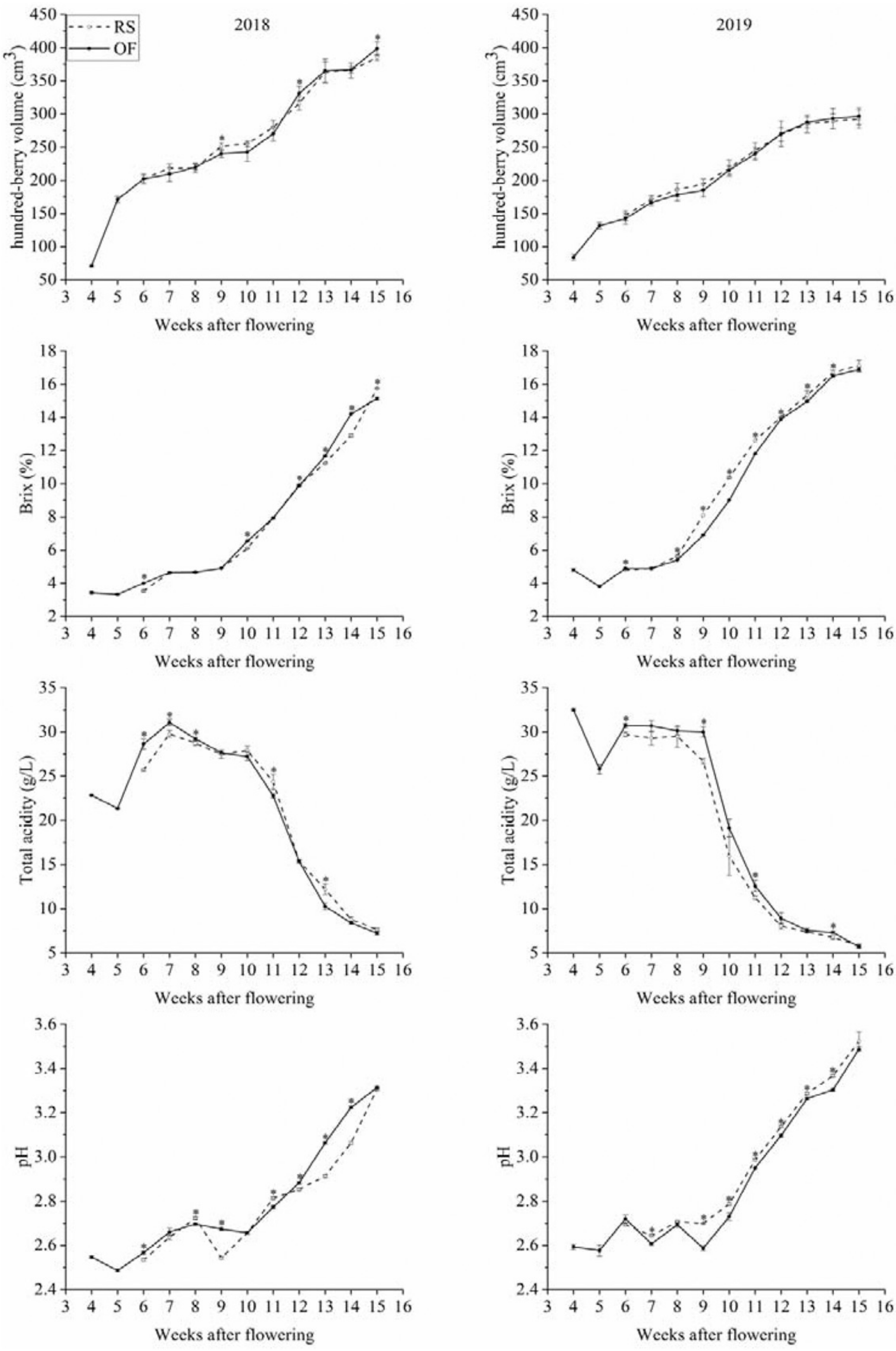

Fig. 2. The basic physical and chemical indicators in Shuijing grape berries under rain-shelter (RS) and open-field (OF) cultivation in 2018 and 2019. *Significant difference in the concentrations of compounds between the RS and OF cultivation ($P < 0.05$). The error bars in these figures indicate the standard deviation (SD).

polytetrafluoroethylene/silicone septa containing a magnetic stirrer and mixed with NaCl (1.0 g) and 4-methyl-2-pentanol (10.00 μL; internal standard solution, 1.017 mg/mL). The mixture was stirred on a heating agitation platform at 40 °C for 30 min using a rotational speed of 250 rpm. Then, a solid phase microextraction manual device (57330-U; Supelco, Bellefonte, PA) with divinylbenzene/carboxen/polydimethylsiloxane fiber (57328-U, Supelco) was used for extraction for 30 min with continued heating and stirring. Finally, the fiber was immediately inserted into the GC injection port to desorb volatiles at 250 °C for 10 min in splitless mode.

The separation and identification of volatiles were determined using an Agilent 7890B GC equipped with an Agilent 5977A MS detector and fitted with a DB-WAX capillary column (length, 60 m; diameter, 0.25 mm; film thickness, 0.25 μm; J&W Scientific, Folsom, CA). The carrier gas was ultrapure helium (99.999%) with a flow rate of 1 mL/min. The temperature program started at 50 °C for 1 min; then, the temperature increased to 220 °C by 3 °C/min, with a final holding time of 5 min. The temperatures of the injector, transfer line, and ion source were set as 250 °C. The mass spectra were obtained using a mass selective detector with electronic impact ionization at 70 eV in full-scan mode with a mass range of 30 to 350 m/z.

Volatile identification was based on matching the mass spectra from the standard national institute of standards and technology (NIST) 2014 library and on retention indices (RIs) of the authenticated standards. When the authenticated standards were not available, tentative identifications were based on the standard NIST 2014 library and a comparison of RIs sourced from NIST Chemistry WebBook (https://webbook.nist.gov/). RIs were calculated using a C_{10}–C_{24} alkane standard mixture (all equally soluble in n-heptane; Sigma, Buchs, Switzerland) under the same chromatographic conditions as those

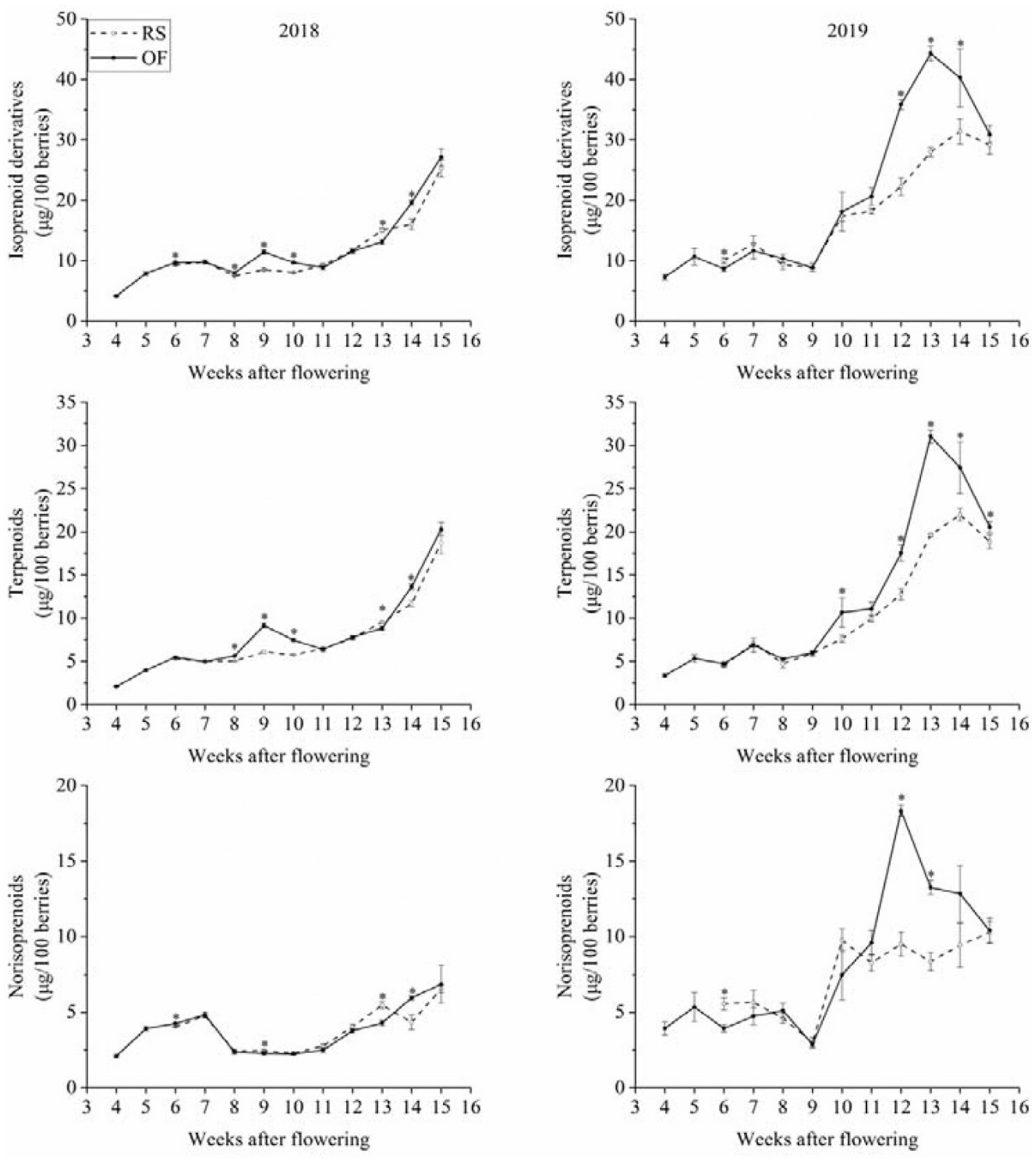

Fig. 3. Accumulation patterns of total isoprenoid-derived volatiles, terpenoids, and norisoprenoids in Shuijing grape berries under rain-shelter (RS) and open-field (OF) cultivation in 2018 and 2019. *Significant difference in the concentrations of compounds between the RS and OF cultivation ($P < 0.05$). The error bars in these figures indicate the standard deviation (SD).

used during the analysis of the Shuijing grape juice.

Volatile quantification was performed by using an internal standard–standard curve method. Standard curves were plotted using the 5-point method. According to the concentrations of sugar and acids in Shuijing grape juice, a synthetic model juice (1.0% volume/volume ethanol content; 150 $g \cdot L^{-1}$ glucose and 5.5 $g \cdot L^{-1}$ tartaric acid; adjusted to a pH of 3.4 with KOH) was prepared. Each authenticated standard was dissolved in ethanol (high-performance liquid chromatography quality) and mixed together; then, this mixed solution was diluted to different levels with the synthetic model juice. The volatile standards of each level were extracted and analyzed under the same chromatographic conditions as those used during the analysis of the Shuijing grape juice.

Additionally, if a volatile that was without a pure standard was identified, then its concentration was estimated by a standard curve of the standard compound that had the most similar chemical structure or was expressed as a relative amount compared with that of the internal standard. The quantitative standard curves of volatiles are listed in Supplemental Table 1.

Statistical analyses. A comparison of means was performed and analyzed using an independent-sample t test with a significance level of $P < 0.05$. The results are presented as the mean ± SD of triplicates. The concentration unit of each compound was expressed as μg per 100 berries. Origin 2018 (OriginLab Corporation, Northampton, MA) was used to construct the graphs and perform the PCA.

Results and Discussion

Physicochemical parameters analysis of Shuijing grape berries

The basic physical and chemical indicators of the Shuijing grape berries grown under RS cultivation and OF cultivation during development (4–15 WAF) in 2018 and 2019 are shown in Fig. 2. RS cultivation had an effect on the 100-berry volumes of the Shuijing grape berries in both vintages. It slightly increased the 100-berry volume before 12 WAF, whereas it decreased the 100-berry volume during 12 to 15 WAF. The TSS values of the Shuijing grape berries cultivated under RS were higher than those of the Shuijing grape berries grown under OF cultivation during development in 2019. This result is consistent

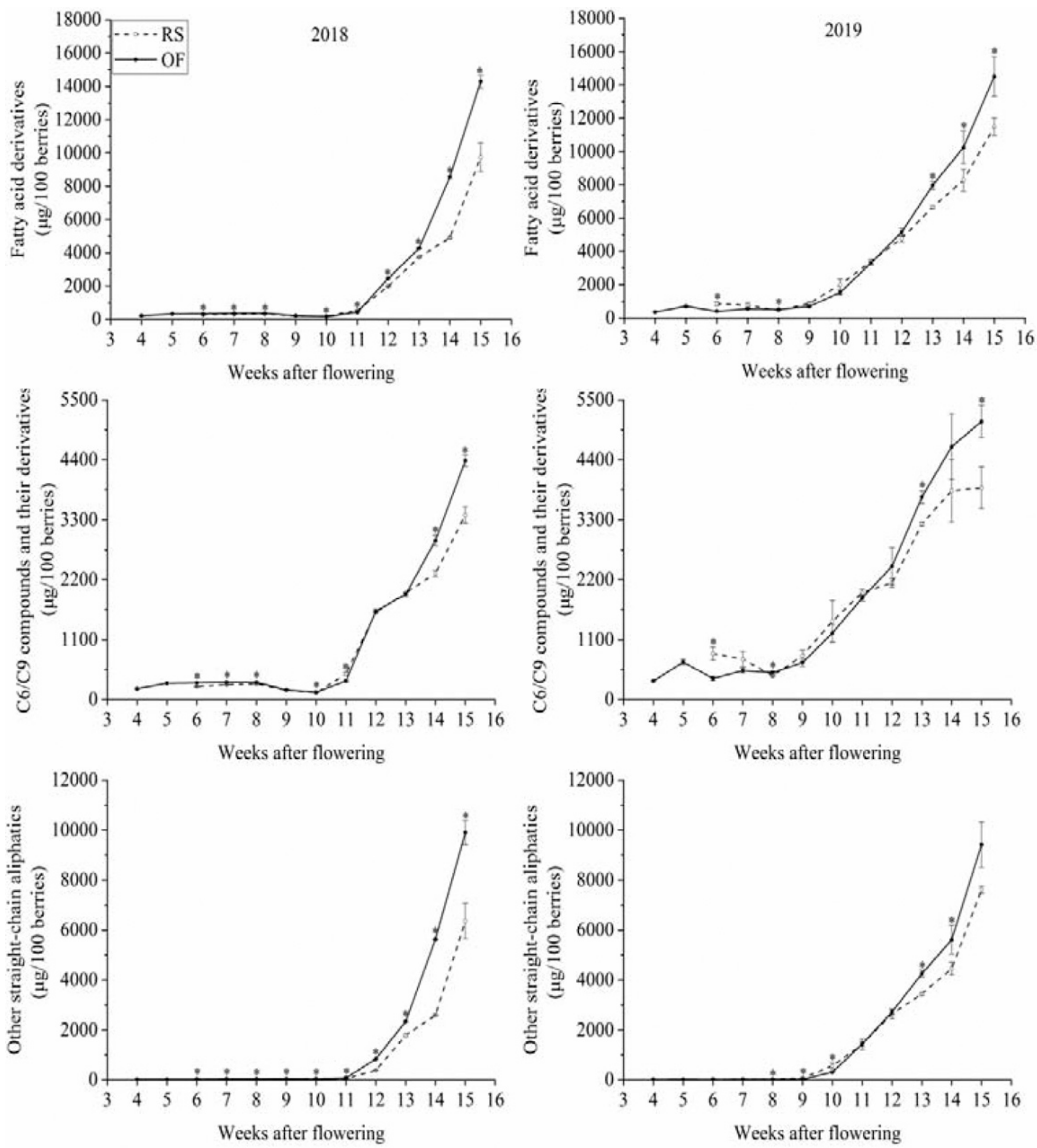

Fig. 4. Accumulation patterns of total fatty acid-derived volatiles, C6/C9 compounds and their derivatives, and the other straight-chain aliphatics in Shuijing grape berries under rain-shelter (RS) and open-field (OF) cultivation in 2018 and 2019. *Significant difference in the concentrations of compounds between the RS and OF cultivation ($P < 0.05$). The error bars in these figures indicate the standard deviation (SD).

with the results reported by Çoban (2007), who observed that applying plastic covering above the grapevines rows had a positive effect on the TSS values of grape berries. However, a higher TSS value of the Shuijing grape berries grown under RS cultivation was only observed at 15 WAF in 2018, which might be explained by the smaller 100-berry volume of the RS sample at this stage. Compared with the OF-cultivated grapes, the RS-cultivated grapes had higher total acidity in 2018 and lower total acidity in 2019. Different impacts of RS cultivation on the total acidity of grape berries have been reported in many studies (Du et al., 2015; Gao et al., 2016; He et al., 2017; Shi et al., 2018). These different results might be related to different varieties, vintages, and/or local climates (Gao et al., 2016). The pH values were generally inversely related to the total acidity values.

Notably, it was observed that the grape berries of the 2019 vintage exhibited a lower 100-berry volume than those of the 2018 vintage. Less rainfall during 9 to 15 WAF and a higher average daily temperature for the 2019 vintage were possibly responsible for this result (Table 1). Smaller grape berries are usually associated with water deficit (Roby and Matthews, 2008) and evaporation. Furthermore, the grape berries of the 2019 vintage showed a greater degree of maturity than those of the 2018 vintage. This result might be attributable to the higher heat accumulation values in 2019, which favored faster ripening of the grape berries (Alessandrini et al., 2017).

Volatile compounds analysis of Shuijing grape berries

To understand the effects of RS cultivation on the accumulation of volatiles in Shuijing grapes, whole berries during development (4–15 WAF) were used for measurements. A total of 95 volatiles in Shuijing grape berries (Supplemental Table 1), 82 in 2018 and 93 in 2019, were identified and quantified during this study. According to the synthetic pathways of their precursors, the volatiles were divided into isoprenoid-derived, fatty acid-derived, amino acid-derived, and other volatiles. The concentrations and accumulation patterns of these four classes of volatiles in

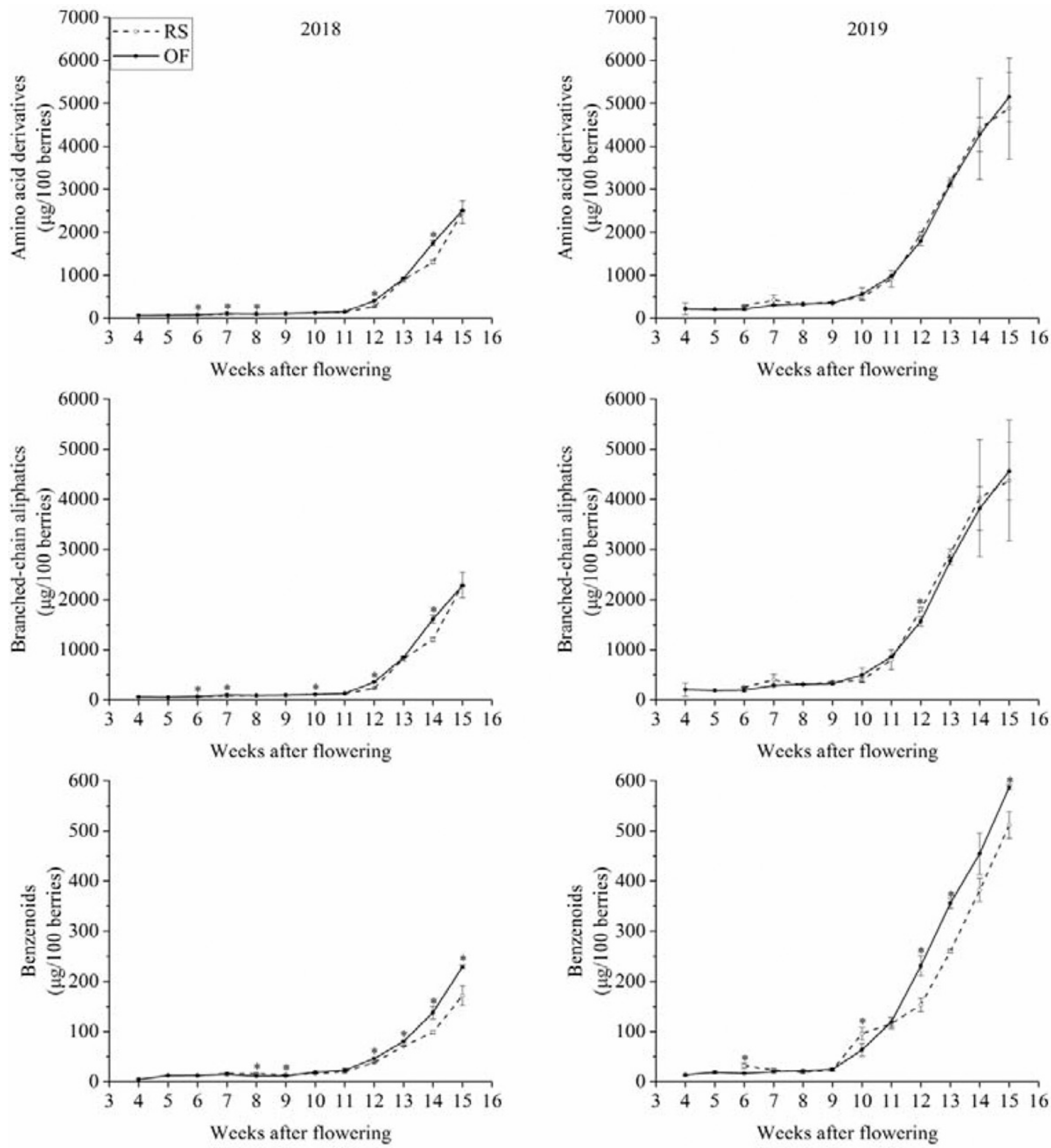

Fig. 5. Accumulation patterns of total amino acid-derived volatiles, branched-chain aliphatics, and benzenoids in Shuijing grape berries under rain-shelter (RS) and open-field (OF) cultivation in 2018 and 2019. *Significant difference in the concentrations of compounds between the RS and OF cultivation ($P < 0.05$). The error bars in these figures indicate the standard deviation (SD).

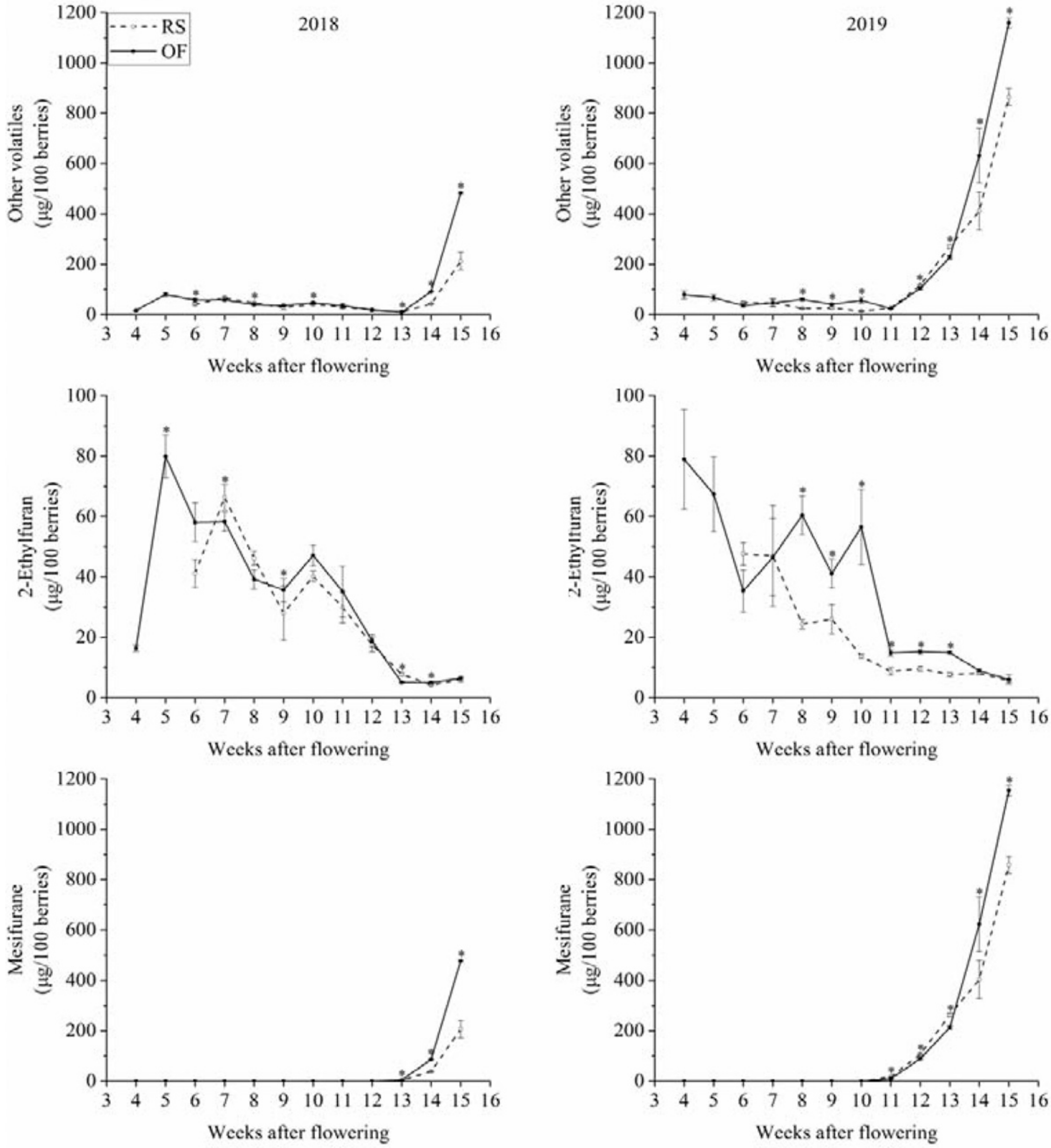

Fig. 6. Accumulation patterns of total other volatiles and 2-ethylfuran and 2,5-dimethyl-4-methoxy-3(2H)-furanone (mesifurane) in Shuijing grape berries under rain-shelter (RS) and open-field (OF) cultivation in 2018 and 2019. *Significant difference in the concentrations of compounds between the RS and OF cultivation ($P < 0.05$). The error bars in these figures indicate the standard deviation (SD).

Shuijing grape berries during development are shown in Supplemental Table 2 and Figs. 3–6. According to these data, RS cultivation affected the accumulation of these volatiles when compared with OF cultivation, especially during 12 to 15 WAF of berry development. This phase is the most important for the biosynthesis, accumulation, and preservation of volatiles in grape berries (Kalua and Boss, 2010), and it is more sensitive to changes in the microclimate, such as changes in the temperature, relative humidity, light, and ultraviolet radiation (Alessandrini et al., 2017; Duan et al., 2019; Liu et al., 2015). Previous studies reported that the structure of the rain shelter had little effect on the temperature and relative humidity of grapevines but clearly reduced the light intensity and ultraviolet radiation (Du et al., 2015; Gao et al., 2016). Therefore, during this study, the differences in light and ultraviolet radiation could be the main reasons for the differences between the volatiles found in RS-cultivated and OF-cultivated Shuijing grapes.

Isoprenoid-derived volatiles. During this study, 14 isoprenoid-derived volatiles (including 8 terpenoids and 6 norisoprenoids) were detected in Shuijing grape berries. The accumulation patterns of terpenoids and norisoprenoids during grape development are shown in Fig. 3. These volatiles were present at low levels in Shuijing grape berries because of the Shuijing grape varietal characteristics. Compared with the grape berries grown under OF cultivation, the grape berries grown under RS cultivation usually contained lower levels of terpenoids and norisoprenoids during development, especially for the samples obtained during 12 to 15 WAF in 2019. This result was probably because the sunshine duration (76.4 h) of this sampling period in 2019 was shorter than that in 2018 (137.5 h), and the shelter further decreased the limited light, resulting in the inhibition of isoprenoid-derived volatiles metabolism. It has been reported that sunlight has a great impact on terpenoids and norisoprenoids by manipulating the light exposure around bunches (Bahena-Garrido et al., 2019; Song et al., 2015). This decreased light intensity greatly reduces the expression of terpene synthase genes (*VvTPS54* and *VvTPS56*) and the production of carotenoids in grapes, which subsequently decreases the concentrations of terpenoids and norisoprenoids (Friedel et al., 2016; Kwasniewski et al., 2010). In terms of individual terpenoids and norisoprenoids, RS

Table 2. Concentrations of volatiles in Shuijing grape berries at 15 weeks after flowering (WAF) under rain-shelter (RS) and open-field (OF) cultivation in 2018 and 2019 (μg/100 berries).

No.	Volatiles	2018 RS	2018 OF	2019 RS	2019 OF
		Isoprenoid-derived volatiles			
	Terpenoids				
a1	α-Pinene	0.36 ± 0.06	0.45 ± 0.08	ND	ND
a2	Eucalyptol	Other	Other	Other	Other
a3	Terpinolene	4.56 ± 0.50	5.03 ± 0.32	3.68 ± 0.49	4.19 ± 0.26
a4	*trans*-Linalool oxide (furanoid)	1.90 ± 0.23	2.04 ± 0.19	4.77 ± 0.53	5.16 ± 0.16
a5	Linalool	6.96 ± 0.49	7.25 ± 0.39	**5.31 ± 0.09**	**5.72 ± 0.15**
a6	Hotrienol	**2.35 ± 0.02**	**2.67 ± 0.01**	1.92 ± 0.12	1.99 ± 0.06
a7	α-Terpineol	**2.64 ± 0.02**	**2.86 ± 0.01**	2.15 ± 0.10	2.48 ± 0.40
a8	Nerol	ND	ND	1.03 ± 0.01	1.03 ± 0.00
	Norisoprenoids				
b1	6-Methyl-5-hepten-2-one	0.14 ± 0.01	0.16 ± 0.01	**0.24 ± 0.05**	**0.34 ± 0.02**
b2	6-Methyl-5-hepten-2-ol	ND	ND	1.53 ± 0.05	1.68 ± 0.10
b3	Theaspirane	ND	ND	3.52 ± 0.32	3.09 ± 0.44
b4	β-Cyclocitral	TR	TR	0.15 ± 0.14	0.69 ± 0.45
b5	(E)-β-Damascenone	6.41 ± 0.27	6.69 ± 1.26	4.83 ± 0.46	4.60 ± 0.43
b6	β-Ionone	Other	Other	Other	Other
	Σ Isoprenoid-derived volatiles	25.29 ± 1.47	27.15 ± 1.41	29.14 ± 1.51	30.97 ± 1.41
		Fatty acid-derived volatiles			
	C6/C9 compounds and their derivatives				
c1	Hexanal	**1174.92 ± 26.05**	**1579.51 ± 71.80**	**770.11 ± 179.73**	**1415.17 ± 283.50**
c2	(Z)-3-Hexenal	**0.56 ± 0.28**	**6.86 ± 0.27**	0.86 ± 0.19	1.53 ± 0.68
c3	(E)-2-Hexenal	**1847.71 ± 48.60**	**2476.28 ± 19.65**	**2047.65 ± 55.97**	**2626.92 ± 167.46**
c4	Ethyl hexanoate	173.73 ± 45.53	108.53 ± 28.04	93.91 ± 41.89	124.44 ± 20.44
c5	Ethyl 3-hexenoate	43.41 ± 9.19	27.08 ± 5.64	39.12 ± 8.41	43.48 ± 8.58
c6	(Z)-3-Hexenyl acetate	Other	Other	Other	Other
c7	Ethyl 2-hexenoate	28.32 ± 7.38	23.73 ± 6.43	33.40 ± 6.92	44.09 ± 9.15
c8	1-Hexanol	**1.24 ± 0.10**	**2.22 ± 0.17**	3.49 ± 1.16	2.81 ± 0.28
c9	(E)-3-Hexen-1-ol	**3.54 ± 0.22**	**4.91 ± 0.07**	3.37 ± 0.60	3.17 ± 0.15
c10	Nonanal	**19.70 ± 1.48**	**23.85 ± 1.00**	44.33 ± 7.73	49.18 ± 4.56
c11	(E,E)-2,4-Hexadienal	3.12 ± 0.52	4.09 ± 0.08	5.76 ± 1.71	5.36 ± 0.20
c12	(E)-2-Hexen-1-ol	**1.30 ± 0.21**	**2.23 ± 0.07**	5.88 ± 1.54	2.84 ± 0.09
c13	3-Nonen-2-one	**12.22 ± 1.60**	**1.64 ± 0.19**	**2.54 ± 0.43**	**1.06 ± 0.10**
c14	1-Nonanol	Other	Other	Other	Other
c15	Hexanoic acid	**76.69 ± 9.74**	**124.26 ± 8.22**	836.22 ± 176.21	782.18 ± 32.23
	Other strain-chain aliphatics				
d1	Methyl acetate	**100.13 ± 7.66**	**129.67 ± 9.14**	120.35 ± 45.48	106.07 ± 5.31
d2	Ethyl acetate	**4738.32 ± 705.98**	**6840.56 ± 227.51**	**4964.70 ± 311.10**	**6825.38 ± 713.84**
d3	Ethyl propionate	**10.81 ± 1.95**	**15.40 ± 1.10**	13.72 ± 3.72	11.93 ± 0.44
d4	2,3-Butanedione	Other	Other	Other	Other
d5	Propyl acetate	**4.24 ± 0.60**	**6.15 ± 0.21**	8.09 ± 1.80	8.11 ± 0.13
d6	Pentanal	TR	TR	TR	TR
d7	Methyl butanoate	1.04 ± 0.13	1.12 ± 0.02	1.01 ± 0.25	0.89 ± 0.19
d8	1-Penten-3-one	**0.90 ± 0.11**	**1.60 ± 0.10**	1.34 ± 0.57	1.49 ± 0.16
d9	Ethyl butanoate	**136.17 ± 25.29**	**88.76 ± 9.26**	91.94 ± 22.46	98.83 ± 10.65
d10	Butyl acetate	1.48 ± 0.13	1.39 ± 0.09	**3.22 ± 0.13**	**1.94 ± 0.14**
d11	2-Pentanol	ND	ND	2.63 ± 0.14	3.03 ± 0.81
d12	3-Penten-2-one	**3.48 ± 0.47**	**2.15 ± 0.22**	ND	ND
d13	Ethyl valerate	**4.50 ± 0.82**	**2.56 ± 0.35**	3.25 ± 0.64	4.68 ± 1.67
d14	Ethyl (E)-2-butenoate	ND	ND	67.85 ± 3.20	71.67 ± 18.25
d15	2-Heptanone	Other	Other	Other	Other
d16	Heptanal	5.39 ± 0.65	4.72 ± 0.43	3.96 ± 0.31	3.38 ± 0.25
d17	Octanal	2.72 ± 0.06	2.81 ± 0.08	**2.68 ± 0.23**	**3.73 ± 0.55**
d18	(Z)-2-Penten-1-ol	5.65 ± 0.17	5.99 ± 0.15	5.67 ± 0.77	4.92 ± 0.33
d19	(E)-2-Heptenal	ND	ND	3.15 ± 0.27	3.20 ± 0.10
d20	Ethyl heptanoate	4.18 ± 1.32	3.41 ± 0.86	5.76 ± 1.99	12.11 ± 4.57
d21	Ethyl (E)-4-heptenoate	0.93 ± 0.37	0.46 ± 0.26	**TR**	**0.95 ± 0.33**
d22	Ethyl octanoate	23.86 ± 2.24	25.59 ± 1.76	13.52 ± 2.24	32.05 ± 14.10
d23	1-Octen-3-ol	**2.08 ± 0.02**	**2.16 ± 0.01**	1.79 ± 0.10	1.82 ± 0.03
d24	1-Heptanol	ND	ND	0.19 ± 0.06	0.19 ± 0.03
d25	Ethyl (Z)-4-octenoate	14.26 ± 2.66	11.12 ± 1.75	11.76 ± 2.71	19.55 ± 5.26
d26	Methyl 3-hydroxybutanoate	**6.18 ± 0.60**	**3.45 ± 0.10**	10.52 ± 2.41	7.76 ± 0.32
d27	(E,E)-2,4-Heptadienal	3.42 ± 0.17	3.71 ± 0.00	2.79 ± 0.15	2.64 ± 0.15
d28	Ethyl 3-hydroxybutanoate	30.48 ± 3.95	28.62 ± 0.58	50.90 ± 12.01	42.83 ± 2.13
d29	Ethyl 2-octenoate	ND	ND	**5.28 ± 1.20**	**10.12 ± 1.60**
d30	1-Octanol	2.89 ± 0.60	2.88 ± 0.34	ND	ND
d31	2R,3S-Butanediol	**1256.80 ± 119.69**	**2707.31 ± 277.23**	2162.78 ± 400.80	2009.10 ± 240.23
d32	Ethyl decanoate	ND	ND	**21.75 ± 1.49**	**29.44 ± 3.05**
d33	Ethyl (E)-4-decenoate	ND	ND	**ND**	**37.75 ± 1.64**
d34	Ethyl (E,Z)-2,4-decadienoate	ND	ND	**30.13 ± 3.67**	**53.99 ± 3.61**
	Σ Fatty acid-derived volatiles	**9746.38 ± 854.56**	**14276.76 ± 383.30**	**11497.39 ± 517.60**	**14511.77 ± 1188.32**

(Continued on next page)

Table 2. (*Continued*)

No.	Volatiles	2018 RS	2018 OF	2019 RS	2019 OF
		Amino acid-derived volatiles			
	Benzenoids				
e1	Toluene	7.22 ± 1.19	8.43 ± 0.85	**13.59 ± 2.08**	**8.19 ± 0.69**
e2	o-Xylene	4.98 ± 1.17	4.06 ± 0.08	**7.17 ± 1.09**	**20.13 ± 4.31**
e3	Styrene	**20.65 ± 5.09**	**11.20 ± 2.14**	7.68 ± 3.99	10.31 ± 2.75
e4	p-Cymene	2.75 ± 0.02	3.05 ± 0.17	5.32 ± 0.90	4.94 ± 0.04
e5	Benzaldehyde	1.57 ± 0.05	1.64 ± 0.10	1.70 ± 0.17	1.57 ± 0.10
e6	Methyl benzoate	1.11 ± 0.62	0.34 ± 0.17	**0.49 ± 0.04**	**0.82 ± 0.11**
e7	Benzeneacetaldehyde	**41.50 ± 1.44**	**54.28 ± 0.87**	**58.76 ± 2.41**	**66.69 ± 3.09**
e8	Acetophenone	**ND**	**8.56 ± 0.51**	25.88 ± 7.23	30.76 ± 0.52
e9	Ethyl benzoate	**ND**	**5.63 ± 0.39**	4.83 ± 0.43	7.27 ± 2.78
e10	4-Ethyl benzaldehyde	Other	Other	Other	Other
e11	Naphthalene	12.42 ± 1.52	12.50 ± 0.86	**2.53 ± 0.44**	**9.32 ± 1.63**
e12	Ethyl phenylacetate	TR	TR	**1.01 ± 0.10**	**1.69 ± 0.08**
e13	3,4-Dimethyl benzaldehyde	**2.06 ± 0.16**	**4.54 ± 0.01**	**2.83 ± 0.17**	**3.69 ± 0.02**
e14	Phenethyl acetate	**1.25 ± 0.01**	**1.34 ± 0.02**	ND	ND
e15	1-(2,4-dimethylphenyl)-ethanone	6.17 ± 0.37	6.37 ± 0.36	**4.33 ± 0.16**	**6.06 ± 0.13**
e16	Benzyl alcohol	ND	ND	3.49 ± 0.10	3.35 ± 0.16
e17	Phenylethyl alcohol	**48.52 ± 9.05**	**83.80 ± 0.35**	342.17 ± 16.80	363.10 ± 6.77
e18	Thymol	**2.78 ± 0.31**	**3.77 ± 0.28**	**2.05 ± 0.25**	**5.83 ± 0.33**
e19	Methyl anthranilate	18.73 ± 0.93	19.27 ± 0.33	**27.33 ± 2.15**	**43.13 ± 1.31**
	Branched-chain aliphatics				
f1	3-Methyl-butanal	117.07 ± 19.12	147.33 ± 4.48	703.43 ± 184.16	499.97 ± 48.24
f2	2-Propanol	2108.74 ± 238.48	2047.57 ± 11.54	3303.84 ± 1012.83	3692.56 ± 542.48
f3	4-Methyl-2-pentanone	**57.59 ± 5.47**	**72.78 ± 0.81**	342.41 ± 13.72	350.93 ± 33.06
f4	2-Methyl-3-buten-2-ol	Other	Other	Other	Other
f5	Isopropyl butanoate	ND	ND	3.77 ± 0.96	2.32 ± 1.37
f6	Ethyl 2-methylbutanoate	**2.81 ± 0.14**	**3.14 ± 0.06**	4.13 ± 0.36	4.26 ± 0.17
f7	Ethyl isovalerate	**0.48 ± 0.09**	**0.31 ± 0.03**	0.87 ± 0.09	1.04 ± 0.07
f8	3-Methyl-1-butanol	ND	ND	4.35 ± 0.18	3.72 ± 1.48
f9	3-Methyl-3-buten-1-ol	Other	Other	Other	Other
f10	3-Methyl-2-buten-1-ol	**2.97 ± 0.08**	**3.75 ± 0.09**	2.59 ± 0.20	2.47 ± 0.25
f11	2-Ethyl-1-hexanol	3.46 ± 0.58	3.13 ± 0.12	**7.76 ± 1.57**	**3.49 ± 0.19**
	Σ Amino acid-derived volatiles	2464.80 ± 269.47	2506.80 ± 10.44	4884.32 ± 1177.75	5147.59 ± 572.67
		Other volatiles			
g1	2-Ethylfuran	6.08 ± 0.80	6.46 ± 0.29	5.61 ± 0.38	6.08 ± 1.46
g2	2,5-Dimethyl-4-methoxy-3(2H)-furanone	**206.12 ± 34.87**	**476.65 ± 4.62**	**858.26 ± 34.30**	**1152.94 ± 20.80**
	Σ Other volatiles	**212.20 ± 35.53**	**483.11 ± 4.37**	**863.87 ± 33.93**	**1159.02 ± 20.07**
	Σ Total volatiles	**12448.68 ± 1134.54**	**17293.83 ± 387.72**	**17274.73 ± 665.75**	**20849.35 ± 1543.03**

ND = not detected; Other = detected during other sampling periods; TR = trace.

Bold indicates that the volatile concentration is statistically significantly different between the Shuijing grape berries under RS and OF cultivation in 2018 and/or 2019 ($P < 0.05$)

cultivation reduced the levels of most of them in Shuijing grape berries sampled at 15 WAF (Table 2).

For the 2018 vintage, an increase was observed in the concentrations of terpenoids and norisoprenoids during development in Shuijing grape berries (Fig. 3), which is in agreement with the results of a study by Alessandrini et al. (2017) of the Glera grape cultivar and the results of a study by Yuan and Qian (2016) of the Pinot noir grape cultivar. For the 2019 vintage, the concentrations of terpenoids and norisoprenoids also exhibited increasing trends during 4 to 11 WAF, but they decreased during 12 to 15 WAF (Fig. 3). This reduction might be attributable to the greater maturity degree of the 2019 grape berries, which would be consistent with the results of several studies of Cabernet Sauvignon, Gewürztraminer and Shiraz grape cultivars (Cramer et al., 2014; Martin et al., 2012; Ribéreau-Gayon et al., 2000; Šuklje et al., 2019). The chemical rearrangements and transformations of the free and bound glycoside forms of volatiles could contribute to the differences in the levels of terpenes and norisoprenoids under different maturity degrees (Šuklje et al., 2019).

Fatty acid-derived volatiles. During this study, 15 C6/C9 compounds and their derivatives and 34 other straight-chain aliphatics (6 straight-chain alcohols, 5 straight-chain aldehydes, 19 straight-chain esters, and 4 straight-chain ketones) were detected in Shuijing grape berries. The accumulation patterns of the C6/C9 compounds and their derivatives and the other straight-chain aliphatics during development are shown in Fig. 4. Their total concentrations remained low before 11 WAF and 9 WAF (2018 and 2019, respectively); then, they dramatically increased until 15 WAF (Fig. 4). The similar variation pattern was also reported previously for the Muscat grape 'Shine Muscat' cultivar (Wu et al., 2020).

As shown in Fig. 4, although the RS cultivation had an impact on the concentrations of the C6/C9 compounds and their derivatives and the other straight-chain aliphatics in Shuijing grape berries during 4 to 11 WAF of both vintages, the grape berries grown under both cultivation methods exhibited similar levels of these volatiles. However, during 12 to 15 WAF, RS cultivation reduced the concentrations of the C6/C9 compounds and their derivatives and the other straight-chain aliphatics, which are products from the degradation of polyunsaturated fatty acids. This might be related to the lower ultraviolet radiation under the shelter (Kobayashi et al., 2011; Meng et al., 2017) that downregulated the metabolism of polyunsaturated fatty acids and their degradation into C6/C9 compounds and their derivatives and other straight-chain aliphatics (Liu et al., 2015). Regarding individual volatiles, hexanal and (E)-2-hexenal exhibited the highest concentrations among the C6/C9 compounds and their derivatives, and their concentrations in RS-cultivated grapes were significantly lower than those in OF-cultivated grapes at 15 WAF of both vintages (Table 2). This result was probably because the RS cultivation affected the expressions of *VviLOXA* (lipoxygenase encoding gene) and *VviHPL1* (hydroperoxide lyase encoding gene), which had a major role in the accumulation of C6 aldehyde (Xu et al., 2015). In grapes, hexanal and (E)-2-hexenal are described as green or leaf-like odors that provide an undesirable flavor perception. Therefore, the RS cultivation might help to alleviate these off-flavor attributes. Regarding the individual other straight-chain aliphatics, ethyl acetate and 2R,3S-butanediol, which are responsible for fruity aromas

(Peinado et al., 2006), were the main volatiles of the other straight-chain aliphatics, and only the concentration of ethyl acetate was decreased by RS cultivating at 15 WAF of both vintages (Table 2).

Amino acid-derived volatiles. During this study, 30 amino acid-derived volatiles, including 19 benzenoids and 11 branched-chain aliphatics, were detected in Shuijing grape berries. The accumulation patterns of benzenoids and branched-chain aliphatics during development are shown in Fig. 5. The concentrations of benzenoids and branched-chain aliphatics changed slightly before 11 WAF and 9 WAF (2018 and 2019, respectively); then, they increased rapidly until 15 WAF (Fig. 5). The similar variation pattern of benzenoids was also reported previously for the Cabernet Sauvignon grape cultivar (Kalua and Boss, 2009; Liu et al., 2015).

As shown in Fig. 5, there was almost no difference in the branched-chain aliphatics in Shuijing grape berries grown under RS and OF cultivation during development of both vintages. It has been reported that the branched-chain aliphatics seem to be unaffected by ultraviolet radiation (Liu et al., 2015). However, RS cultivation decreased the concentration of benzenoids during 12 to 15 WAF of both vintages. It has been demonstrated that lowering ultraviolet radiation could reduce the production of phenylalanine-derived volatiles (e.g., benzenoids) from the shikimate pathway (Gao et al., 2016). Therefore, the attenuation of ultraviolet radiation under RS treatment might be one of the most important factors resulting in the decrease of the concentration of benzenoids in Shuijing grape berries. Phenylethyl alcohol, benzeneacetaldehyde, and methyl anthranilate were the major benzenoids in Shuijing grape berries at 15 WAF (Table 2), and their concentrations were reduced by RS cultivation in the grapes of both vintages, most notably benzeneacetaldehyde. This result is similar to the results of a study by Gao et al. (2016), who found that RS cultivation could significantly decrease the level of benzeneacetaldehyde in Chardonnay grape berries. 3-Methyl-butanal and 2-propanol accounted for more than 80% of the total concentration of branched-chain aliphatics in Shuijing grape berries at 15 WAF, but no differences in their concentrations were found between the grapes grown under RS and OF cultivation of either vintage (Table 2).

Other volatiles. During this study, 2-ethylfuran and 2,5-dimethyl-4-methoxy-3(2H)-furanone (mesifurane) were detected in Shuijing grape berries. The accumulation patterns of 2-ethylfuran and 2,5-dimethyl-4-methoxy-3(2H)-furanone (mesifurane) during development are shown in Fig. 6. The concentration of 2-ethylfuran in Shuijing grape berries showed a substantial decrease during grape development, and it accounted for only a small proportion of other volatiles when the grapes were ripe (Fig. 6). According to the data, the concentration of 2-ethylfuran in RS-cultivated grapes was lower than that in OF-cultivated grapes during development, most notably in the grapes of the 2019 vintage. Mesifurane was only detected during the late stage of berry development (13–15 WAF in 2018; 11–15 WAF in 2019), and its concentration was reduced by RS cultivation at 14 and 15 WAF of both vintages. Many studies reported that mesifurane was evidently synthesized from fructose (Kallio, 1975; Song et al., 2016; Wein et al., 2001), which was described as sweet, spicy, cherry-like, and earth-flavored (Kallio, 2018). Fu et al. (2017) revealed that light greatly affected the biosynthesis of mesifurane in strawberries. However, the synthesis mechanism of mesifurane in grapes is still unclear, and further research is needed.

It is worth noting that the rapid accumulation of isoprenoid-derived, fatty acid-derived, amino acid-derived and other volatiles occurred 2 weeks earlier during berry development in 2019 than in 2018. Additionally, higher concentrations of benzenoids, branched-chain aliphatics, and mesifurane in grape berries were detected in 2019 than in 2018. These data could be correlated with the higher heat accumulation values in 2019, which favored the faster grape ripening and volatile accumulation in the grape berries (Alessandrini et al., 2017). Furthermore, sunshine duration during 12 to 15 WAF was lower in 2019 than that in 2018. Previous studies reported that lower light exposure increased the concentrations of benzenoids (Wang et al., 2019).

Principal component analysis

To understand the influences of the vintage and cultivation methods on the physicochemical parameters and volatiles of Shuijing grape berries, the PCA was performed using all the physicochemical parameters and volatiles of each berry sample collected during 2018 and 2019 under RS and OF cultivation.

Figure 7 shows the PCA of the physicochemical parameters of all the Shuijing grape berry samples. The first two components accounted for 96.9% of the total variance. The first component (PC1) accounted for 88.0% of the total variance, and the berry samples were distributed from the negative to the positive axis of PC1, corresponding to the grape developmental stages. The second component (PC2) accounted for 8.9% of the total variance, and the berry samples collected in 2018 (except for 18 OF-4 and 18 OF-5) and 2019 corresponded to the positive and negative axes of PC2, respectively. This is mainly because the grape berries of the 2018 vintage were characterized by a higher 100-berry volume, whereas the grape berries of the 2019 vintage were characterized by higher values of TSS and pH. However, based on their physicochemical parameters, the grape berries under RS and OF cultivation could not be clearly differentiated by PC1 and PC2. Therefore, the physicochemical parameters of the Shuijing grape berries were more greatly affected by the vintage than by the cultivation method.

Figure 8 shows the PCA of the volatiles of all the Shuijing grape berry samples. The first two principal components accounted for 70.6% of the total variance, whereby 58.8% and 11.8% of the variance were accounted for by PC1 and PC2, respectively. From the loading plot, it was observed that a majority of volatiles loaded onto the positive axis of PC1 (the first and fourth quadrants), and these volatiles exhibited higher concentrations in

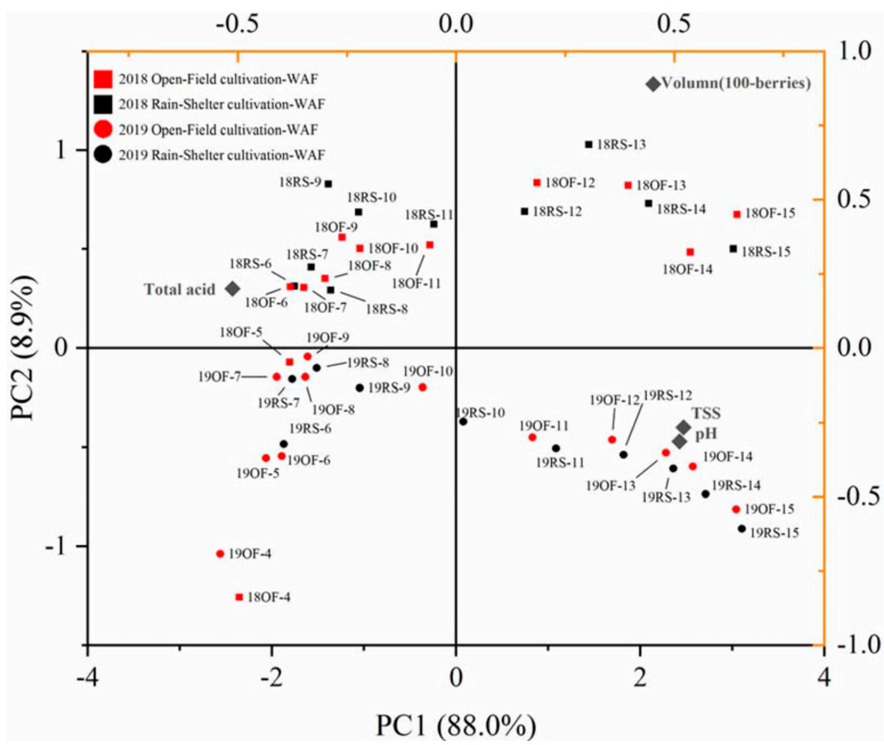

Fig. 7. Principal component analysis of physicochemical parameters in Shuijing grape berries during development in 2018 and 2019.

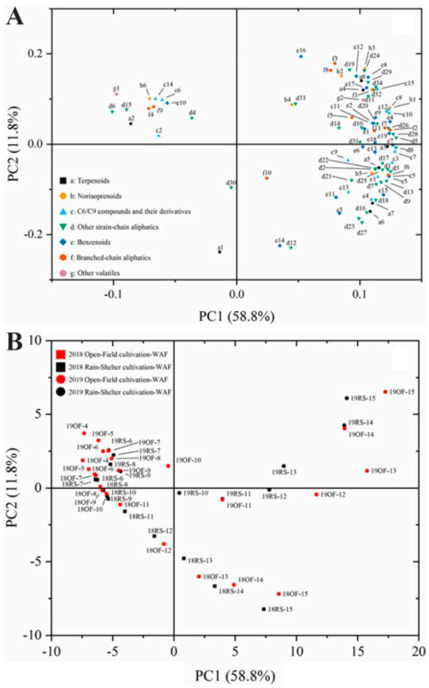

Fig. 8. Principal component analysis of volatiles in Shuijing grape berries during development in 2018 and 2019. (**A**) Principal component loading plot. (**B**) Principal component scatter plot.

Shuijing grape berries collected during 12 to 15 WAF. The volatiles loaded onto the negative axis of PC1 (the second and third quadrants) were generally detected in Shuijing grape berries collected during 4 to 11 WAF. Because of the influence of different vintages, the Shuijing grape berries of the 2018 vintage were clearly separated from those of the 2019 vintage in accordance with PC2, especially those samples collected during 12 to 15 WAF. Similar to the PCA of the physicochemical parameters, the grape berries of either vintage were not clearly differentiated according to their cultivation methods.

In conclusion, RS cultivation had no effect on the accumulation patterns of the volatiles, but it affected the concentrations of the volatiles in Shuijing grape berries during development, especially during the berry maturation phase. The concentrations of isoprenoid-derived volatiles (2019), fatty acid-derived volatiles, and amino acid-derived benzenoids in Shuijing grape berries were reduced by RS cultivation during maturation. The reduction in volatiles might be because of the decreased intensity of visible light and ultraviolet radiation caused by RS cultivation. Additionally, the results of the PCA indicated that the vintage had a much greater impact on the physicochemical parameters and volatiles of the Shuijing grape berries compared with the cultivation method. Because of the higher heat accumulation values/GDD_{10}, the Shuijing grape berries of the 2019 vintage exhibited a greater maturity degree (higher TSS values and lower total acidity) and contained higher concentrations of total and some individual volatiles than those of the 2018 vintage. The present study provided new knowledge regarding the formation and accumulation patterns of volatiles in Shuijing grape berries under RS cultivation and has significance for exploring the potential of RS cultivation in grape-producing regions with excessive rainfall. Further transcriptional analysis of volatile synthesis genes will provide a better understanding of the effects of RS cultivation on the accumulation of volatiles in Shuijing grape berries. Moreover, the synthesis mechanism of 2,5-dimethyl-4-methoxy-3(2H)-furanone (mesifurane) in grapes is still unclear, and further research is needed.

Literature Cited

Alessandrini, M., F. Gaiotti, N. Belfiore, F. Matarese, C. D'Onofrio, and D. Tomasi. 2017. Influence of vineyard altitude on Glera grape ripening (*Vitis vinifera* L.): Effects on aroma evolution and wine sensory profile. J. Sci. Food Agr. 97:2695–2705, https://doi.org/10.1002/jsfa.8093.

Bahena-Garrido, S.M., T. Ohama, Y. Suehiro, Y. Hata, A. Isogai, K. Iwashita, N. Goto-Yamamoto, and K. Koyama. 2019. The potential aroma and flavor compounds in vitis sp. cv. koshu and v. vinifera l. cv. chardonnay under different environmental conditions. J. Sci. Food Agr. 99:1926–1937, https://doi.org/10.1101/383000.

Bureau, S.M., A.J. Razungles, and R.L. Baumes. 2010. The aroma of Muscat of Frontignan grapes: Effect of the light environment of vine or bunch on volatiles and glycoconjugates. J. Sci. Food Agr. 80:2012–2020, https://doi.org/10.1002/1097-0010(200011)80:14<2012:AID-JSFA738>3.0.CO;2-X.

Chavarria, G., H.P. de Santos, O.R. Sônego, G.A.B. Marodin, H. Bergamaschi, and L.S. Cardoso. 2007. Incidence of diseases and needs of control in overhead covered grapes. Rev. Bras. Frutic. 29:477–482, https://doi.org/10.1590/S0100-29452007000300014.

Çoban, H. 2007. Effects of plastic covering on yield, physical and chemical characteristics of some table grapes (*Vitis vinifera* L.). Asian J. Chem. 19:4052–4058.

Cramer, G.R., R. Ghan, K.A. Schlauch, R.L. Tillett, H. Heymann, A. Ferrarini, M. Delledonne, S. Zenoni, M. Fasoli, and M. Pezzotti. 2014. Transcriptomic analysis of the late stages of grapevine (*Vitis vinifera* cv. Cabernet Sauvignon) berry ripening reveals significant induction of ethylene signaling and flavor pathways in the skin. BMC Plant Biol. 14:370, https://doi.org/10.1186/s12870-014-0370-8.

Du, F., W.P. Deng, M. Yang, H.N. Wang, R.Z. Mao, J.H. Shao, J.X. Fan, Y.D. Chen, Y. Fu, C.Y. Li, X.H. He, Y.Y. Zhu, and S.S. Zhu. 2015. Protecting grapevines from rainfall in rainy conditions reduces disease severity and enhances profitability. Crop Prot. 67:261–268, https://doi.org/10.1016/j.cropro.2014.10.024.

Duan, B.B., C.Z. Song, Y.M. Zhao, Y. Jiang, P.B. Shi, J.F. Meng, and Z.W. Zhang. 2019. Dynamic changes in anthocyanin biosynthesis regulation of Cabernet Sauvignon (*Vitis vinifera* L.) grown during the rainy season under rain-shelter cultivation. Food Chem. 283:404–413, https://doi.org/10.1016/j.foodchem.2018.12.131.

Dudareva, N., E. Pichersky, and J. Gershenzon. 2004. Biochemistry of plant volatiles. Plant Physiol. 135:1893–1902, https://doi.org/10.2307/4356546.

Dunlevy, J.D., K.L. Soole, M.V. Perkins, E.G. Dennis, R.A. Keyzers, C.M. Kalua, and P.K. Boss. 2010. Two *O*-methyltransferases involved in the biosynthesis of methoxypyrazines: Grape-derived aroma compounds important to wine flavour. Plant Mol. Biol. 74:77–89, https://doi.org/10.1007/s11103-013-0012-9.

Friedel, M., J. Frotscher, M. Nitsch, M. Hofmann, J. Bogs, M. Stoll, and H. Dietrich. 2016. Light promotes expression of monoterpene and flavonol metabolic genes and enhances flavour of winegrape berries (*Vitis vinifera* L. cv. Riesling). Aust. J. Grape Wine Res. 22:409–421, https://doi.org/10.1111/ajgw.12229.

Fu, X.M., S.H. Cheng, Y.Q. Zhang, B. Du, C. Feng, Y. Zhou, X. Mei, Y.M. Jiang, X.W. Duan, and Z.Y. Yang. 2017. Differential responses of four biosynthetic pathways of aroma compounds in postharvest strawberry (*Fragaria ×ananassa* Duch.) under interaction of light and temperature. Food Chem. 221:356–364, https://doi.org/10.1016/j.foodchem.2016.10.082.

Gao, Y., X.X. Li, M.M. Han, X.F. Yang, Z. Li, J. Wang, and Q.H. Pan. 2016. Rain-shelter cultivation modifies carbon allocation in the polyphenolic and volatile metabolism of *Vitis vinifera* L. Chardonnay Grapes. PLoS One 11:0156117, https://doi.org/10.1371/journal.pone.0156117.

Gómez-Míguez, M.J., M. Gómez-Míguez, I.M. Vicario, and F.J. Heredia. 2007. Assessment of colour and aroma in white wines vinifications: Effects of grape maturity and soil type. J. Food Eng. 79:758–764, https://doi.org/10.1016/j.jfoodeng.2006.02.038.

He, Y.N., P.F. Ning, T.X. Yue, and Z.W. Zhang. 2017. Volatile profiles of Cabernet Gernischet wine under rain-shelter cultivation and open-field cultivation using solid-phase microextraction–gas chromatography/mass spectrometry. Int. J. Food Prop. 20:2181–2196, https://doi.org/10.1080/10942912.2016.1174711.

Kallio, H. 1975. Identification of volatile aroma compounds in arctic bramble, *Rubus arcticus* L., and their development during the ripening of the berry, with special reference to *Rubus stellatus* Sm. University of Turku, Turku, PhD Diss.

Kallio, H.P. 2018. Historical review on the identification of mesifurane, 2,5-dimethyl-4-methoxy-3(2h)-furanone, and its occurrence in berries and fruits. J. Agr. Food Chem. 66:2553–2560, https://doi.org/10.1021/acs.jafc.8b00519.

Kalua, C.M. and P.K. Boss. 2009. Evolution of volatile compounds during the development of Cabernet Sauvignon grapes (*Vitis vinifera* L.). J. Agr. Food Chem. 57:3818–3830, https://doi.org/10.1021/jf803471n.

Kalua, C.M. and P.K. Boss. 2010. Comparison of major volatile compounds from Riesling and Cabernet Sauvignon grapes (*Vitis vinifera L.*) from fruitset to harvest. Aust. J. Grape Wine Res. 16:337–348, https://doi.org/10.1111/j.1755-0238.2010.00096.x.

Kobayashi, H., H. Takase, Y. Suzuki, F. Tanzawa, R. Takata, K. Fujita, M. Kohno, M. Mochizuki, S. Suzuki, and T. Konno. 2011. Environmental stress enhances biosynthesis of flavor precursors, S-3-(hexan-1-ol)-glutathione and S-3-(hexan-1-ol)-L-cysteine, in grapevine through glutathione S-transferase activation. J. Expt. Bot. 62:1325–1336, https://doi.org/10.1093/jxb/erq376.

Koyama, K. and N. Goto-Yamamoto. 2008. Bunch shading during different developmental stages affects the phenolic biosynthesis in berry skins of 'Cabernet Sauvignon' grapes. J. Amer. Soc.

Hort. Sci. 133:743–753, https://doi.org/10.1002/anie.201309746.
Kwasniewski, M.T., J.E.V. Heuvel, B.S. Pan, and G.L. Sacks. 2010. Timing of cluster light environment manipulation during grape development affects C_{13} norisoprenoid and carotenoid concentrations in Riesling. J. Agr. Food Chem. 58:6841–6849, https://doi.org/10.1021/jf904555p.
Li, B.B., J.F. Jiang, X.C. Fan, Y. Zhang, H.S. Sun, G.H. Zhang, and C.H. Liu. 2017. Molecular characterization of Chinese grape Landraces (*Vitis* L.) using microsatellite DNA markers. HortScience 52:533–540, https://doi.org/10.21273/hortsci11802-17.
Li, X.X., F. He, J. Wang, Z. Li, and Q.H. Pan. 2014. Simple rain-shelter cultivation prolongs accumulation period of anthocyanins in wine grape berries. Molecules 19:14843–14861, https://doi.org/10.3390/molecules190914843.
Liu, D., Y. Gao, X.X. Li, Z. Li, and Q.H. Pan. 2015. Attenuated UV radiation alters volatile profile in cabernet sauvignon grapes under field conditions. Molecules 20:16946–16969, https://doi.org/10.3390/molecules200916946.
Lund, S.T. and J. Bohlmann. 2006. The molecular basis for wine grape quality-A volatile subject. Science 311:804–805, https://doi.org/10.1126/science.1118962.
Martin, D.M., A. Chiang, S.T. Lund, and J. Bohlmann. 2012. Biosynthesis of wine aroma: Transcript profiles of hydroxymethylbutenyl diphosphate reductase, geranyl diphosphate synthase, and linalool/nerolidol synthase parallel monoterpenol glycoside accumulation in Gewürztraminer grapes. Planta 236:919–929, https://doi.org/10.1007/s00425-012-1704-0.
Meng, J.F., P.F. Ning, T.F. Xu, and Z.W. Zhang. 2013. Effect of rain-shelter cultivation of *vitis vinifera* cv. Cabernet Gernischet on the phenolic profile of berry skins and the incidence of grape diseases. Molecules 18:381–397, https://doi.org/10.3390/molecules18010381.
Meng, N., Z.Y. Ren, X.F. Yang, and Q.H. Pan. 2017. Effects of simple rain-shelter cultivation on fatty acid and amino acid accumulation in 'Chardonnay' grape berries. J. Sci. Food Agr. 98:1222–1231, https://doi.org/10.1002/jsfa.8593.
Noguerol-Pato, R., C. González-Barreiro, B. Cancho-Grande, M.C. Martínez, J.L. Santiago, and J. Simal-Gándara. 2012. Floral, spicy and herbaceous active odorants in Gran Negro grapes from shoulders and tips into the cluster, and comparison with Brancellao and Mouratón varieties. Food Chem. 135:2771–2782, https://doi.org/10.1016/j.foodchem.2012.06.104.
Peinado, R. A., J. C. Mauricio, J. Moreno. 2006. Aromatic series in sherry wines with gluconic acid subjected to different biological aging conditions by *Saccharomyces cerevisiae var. capensis*. Food Chem. 94:232–239, https://doi.org/10.1016/j.foodchem.2004.11.010.
Ribéreau-Gayon, P., Y. Glories, A. Maujean, and D. Dubourdieu. 2000. Varietal Aroma, p. 205-230. In C. Rychlewski (ed.). Handbook of enology volume 2: The chemistry of wine and stabilization and treatments. 2nd ed. John Wiley & Sons Ltd Press, Chichester, England.
Roby, G. and M.A. Matthews. 2008. Relative proportions of seed, skin and flesh, in ripe berries from cabernet sauvignon grapevines grown in a vineyard either well irrigated or under water deficit. Aust. J. Grape Wine Res. 10:74–82, https://doi.org/10.1111/j.1755-0238.2004.tb00009.x.
Shi, P.B., L.L. Zuo, M.Y. Liu, C.Z. Song, Z.W. Zhang, and J.F. Meng. 2018. Berry anthocyanin content of Cabernet Sauvignon (*Vitis Vinifera* L.) cultivated under rain-shelter systems with different coloured plastic films. J. Hort. Sci. Biotechnol. 93:8–18, https://doi.org/10.1080/14620316.2017.1343102.
Song, C.K., X.T. Hong, S. Zhao, J.Y. Liu, K. Schulenburg, F.C. Huang, K. Franz-Oberdorf, and W. Schwab. 2016. Glucosylation of 4-hydroxy-2,5-dimethyl-3(2*H*)-furanone, the key strawberry flavor compound in strawberry fruit. Plant Physiol. 171:139–151, https://doi.org/10.1104/pp.16.00226.
Song, J.Q., R. Smart, H. Wang, B. Dambergs, A. Sparrow, and M.C. Qian. 2015. Effect of grape bunch sunlight exposure and UV radiation on phenolics and volatile composition of *Vitis vinifera* L. cv. Pinot noir wine. Food Chem. 173:424–431, https://doi.org/10.1016/j.foodchem.2014.09.150.
Šuklje, K., S. Carlin, J. Stanstrup, G. Antalick, J.W. Blackman, C. Meeks, A. Deloire, L.M. Schmidtke, and U. Vrhovsek. 2019. Unravelling wine volatile evolution during Shiraz grape ripening by untargeted HS-SPME-GC × GC-TOFMS. Food Chem. 277:753–765, https://doi.org/10.1016/j.foodchem.2018.10.135.
Wang, Y., Y.N. He, L. He, F. He, W. Chen, C.Q. Duan, and J. Wang. 2019. Changes in global aroma profiles of cabernet sauvignon in response to cluster thinning. Food Res. Int. 122:56–65, https://doi.org/10.1016/j.foodres.2019.03.061.
Wein, M., E. Lewinsohn, and W. Schwab. 2001. Metabolic fate of isotopes during the biological transformation of carbohydrates to 2,5-dimethyl-4-hydroxy-3(2*H*)-furanone in strawberry fruits. J. Agr. Food Chem. 49:2427–2432, https://doi.org/10.1021/jf010072p.
Wu, Y.S., S.Y. Duan, L.P. Zhao, Z. Gao, M. Luo, S.R. Song, W.P. Xu, C.X. Zhang, C. Ma, and S.P. Wang. 2016. Aroma characterization based on aromatic series analysis in table grapes. Sci. Rep. 6:31116, https://doi.org/10.1038/srep31116.
Wu, Y.S., W.W. Zhang, S.R. Song, W.P. Xu, C.X. Zhang, C. Ma, L. Wang, and S.P. Wang. 2020. Evolution of volatile compounds during the development of Muscat grape 'Shine Muscat' (*Vitis labrusca* × *V. vinifera*). Food Chem. 309:125778, https://doi.org/10.1016/j.foodchem.2019.125778.
Xu, X.Q., B. Liu, B.Q. Zhu, Y.B. Lan, Y. Gao, D. Wang, M.J. Reeves, and C.Q. Duan. 2015. Differences in volatile profiles of Cabernet Sauvignon grapes grown in two distinct regions of China and their responses to weather conditions. Plant Physiol. Biochem. 89:123–133, https://doi.org/10.1016/j.plaphy.2015.02.020.
Yuan, F. and M.C. Qian. 2016. Development of C_{13}-norisoprenoids, carotenoids and other volatile compounds in *Vitis vinifera* L. Cv. Pinot noir grapes. Food Chem. 192:633–641, https://doi.org/10.1016/j.foodchem.2015.07.050.

Supplemental Table 1. Quantitative standards and standard curves for quantification of volatiles in Shuijing grape berries.

No.	Volatiles	CAS	RT[z]	RI[y]	Identification[x]	Quantitative standards	Standard curves[w]	R^2
1	Methyl acetate	000079-20-9	5.62	874	A	Methyl acetate	y = 13354.40x − 4.77	0.999
2	Ethyl acetate	000141-78-6	6.38	908	A	Ethyl acetate	y = 4041.08x − 0.55	0.999
3	3-Methyl-butanal	000590-86-3	6.93	932	A	3-Methyl-butanal	y = 549386.99x − 23.83	0.996
4	2-Propanol	000067-63-0	7.09	939	A	2-Propanol	y = 131715.25x + 12.36	0.997
5	2-Ethylfuran	003208-16-0	7.60	962	A	2-Ethylfuran	y = 6640.52x + 0.29	0.999
6	Ethyl propionate	000105-37-3	7.70	966	A	Ethyl propionate	y = 1727.58x−5.97	0.999
7	2,3-Butanedione	000431-03-8	8.07	981	B		*y = 2034x	
8	Propyl acetate	000109-60-4	8.08	982	A	Propyl acetate	y = 1148.46x − 0.04	0.998
9	Pentanal	000110-62-3	8.22	988	B	Hexanal	y = 1205.48x − 3.51	0.999
10	Methyl butanoate	000623-42-7	8.35	993	A	Methyl butanoate	y = 935.52x + 0.76	0.990
11	4-Methyl-2-pentanone	000108-10-1	8.94	1011	B		*y = 2034x	
12	1-Penten-3-one	001629-58-9	9.30	1022	B		*y = 2034x	
13	α-Pinene	000080-56-8	9.43	1025	B		*y = 2034x	
14	Ethyl butanoate	000105-54-4	9.72	1034	A	Ethyl butanoate	y = 752.83x + 4.12	0.994
15	2-Methyl-3-buten-2-ol	000115-18-4	9.78	1035	B		*y = 2034x	
16	Isopropyl butanoate	000638-11-9	9.80	1036	B		*y = 2034x	
17	Toluene	000108-88-3	9.92	1040	B	p-Cymene	y = 4174.67x + 4.91	0.997
18	Ethyl 2-methylbutanoate	007452-79-1	10.21	1049	A	Ethyl 2-methylbutanoate	y = 773.09x + 5.44	0.998
19	Ethyl isovalerate	000108-64-5	10.67	1062	A	Ethyl isovalerate	y = 674.87x + 0.31	0.969
20	Butyl acetate	000123-86-4	10.81	1066	A	Butyl acetate	y = 733.13x + 1.87	0.997
21	Hexanal	000066-25-1	11.16	1079	A	Hexanal	y = 1205.48x − 3.51	0.999
22	2-pentanol	006032-29-7	12.46	1115	B	3-Methyl-1-butanol	y = 4120.79x − 1.85	0.999
23	3-Penten-2-one	000625-33-2	12.78	1125	B		*y = 2034x	
24	Ethyl valerate	000539-82-2	13.01	1132	A	Ethyl valerate	y = 737.43x + 1.64	0.998
25	(Z)-3-Hexenal	004440-65-7	13.30	1140	B	Hexanal	y = 1205.48x − 3.51	0.999
26	Ethyl (E)-2-butenoate	000623-70-1	14.14	1165	B	Ethyl butanoate	y = 752.83x + 4.12	0.994
27	2-Heptanone	000110-43-0	14.90	1188	B		*y = 2034x	
28	Heptanal	000111-71-7	14.98	1190	A	Heptanal	y = 782.16x + 6.07	0.999
29	o-Xylene	000095-47-6	15.03	1191	B	p-Cymene	y = 4174.67x + 4.91	0.997
30	3-Methyl-1-butanol	000123-51-3	15.92	1214	A	3-Methyl-1-butanol	y = 4120.79x − 1.85	0.999
31	Eucalyptol	000470-82-6	16.17	1220	B		*y = 2034x	
32	(E)-2-Hexenal	006728-26-3	16.52	1229	B	Hexanal	y = 1205.48x − 3.51	0.999
33	Ethyl hexanoate	000123-66-0	16.93	1239	A	Ethyl hexanoate	y = 1415.88x + 2.30	0.996
34	3-Methyl-3-buten-1-ol	000763-32-6	17.63	1255	A	3-Methyl-3-buten-1-ol	y = 3336.14x + 6.03	0.998
35	Styrene	000100-42-5	17.99	1263	A	Styrene	y = 9310.03x + 0.18	0.988
36	p-Cymene	000099-87-6	18.56	1277	A	p-Cymene	y = 4174.67x + 4.91	0.997
37	Terpinolene	000586-62-9	19.12	1290	B		*y = 2034x	
38	Octanal	000124-13-0	19.30	1294	B	Heptanal	y = 782.16x + 6.07	0.999
39	Ethyl 3-hexenoate	002396-83-0	19.78	1306	B	Ethyl hexanoate	y = 1415.88x + 2.30	0.996
40	(Z)-3-Hexenyl acetate	003681-71-8	20.47	1322	B		*y = 2034x	
41	(Z)-2-Penten-1-ol	001576-95-0	20.61	1326	B	(Z)-2-Hexen-1-ol	y = 1426.74x + 11.50	0.996
42	3-Methyl-2-buten-1-ol	000556-82-1	20.71	1328	B	3-Methyl-3-buten-1-ol	y = 3336.14x + 6.03	0.998
43	(E)-2-Heptenal	018829-55-5	20.87	1332	B	Heptanal	y = 782.16x + 6.07	0.999
44	Ethyl heptanoate	000106-30-9	21.17	1339	A	Ethyl heptanoate	y = 3730.19x − 2.30	0.980
45	6-Methyl-5-hepten-2-one	000110-93-0	21.39	1344	A	6-Methyl-5-hepten-2-one	y = 163.20x + 0.15	0.999
46	Ethyl 2-hexenoate	001552-67-6	21.73	1352	B	Ethyl hexanoate	y = 1415.88x + 2.30	0.996
47	1-Hexanol	000111-27-3	22.04	1359	A	1-Hexanol	y = 524.82x − 0.17	0.999
48	Ethyl (E)-4-heptenoate	054340-70-4	23.12	1385	B	Ethyl heptanoate	y = 3730.19x − 2.30	0.980
49	(E)-3-Hexen-1-ol	000928-96-1	23.41	1392	A	(E)-3-Hexen-1-ol	y = 1524.25x + 4.03	0.999
50	Nonanal	000124-19-6	23.76	1400	A	Nonanal	y = 5996.88x + 32.97	0.999
51	(E,E)-2,4-Hexadienal	000142-83-6	24.22	1411	B	Hexanal	y = 1205.48x − 3.51	0.999
52	(E)-2-Hexen-1-ol	000928-95-0	24.31	1414	A	(E)-2-Hexen-1-ol	y = 1099.76x − 0.70	0.999
53	Ethyl octanoate	000106-32-1	25.47	1442	A	Ethyl octanoate	y = 3657.96x + 1.74	0.997
54	*trans*-Linalool oxide (furanoid)	034995-77-2	26.01	1455	B		*y = 2034x	
55	1-Octen-3-ol	003391-86-4	26.11	1457	A	1-Octen-3-ol	y = 163.31 + 4.92	0.999
56	1-Heptanol	000111-70-6	26.40	1464	A	1-Heptanol	y = 200.40x − 0.18	0.999
57	6-Methyl-5-hepten-2-ol	001569-60-4	26.67	1471	B		*y = 2034x	
58	Ethyl (Z)-4-octenoate	034495-71-1	27.25	1485	B	Ethyl octanoate	y = 3657.96x + 1.74	0.997
59	Methyl 3-hydroxybutanoate	001487-49-6	27.57	1493	B	Methyl butanoate	y = 935.52x + 0.76	0.990
60	2-Ethyl-1-hexanol	000104-76-7	27.82	1498	A	2-Ethyl-1-hexanol	y = 131.68x + 0.98	0.999
61	(E,E)-2,4-Heptadienal	004313-03-5	28.05	1504	B	Heptanal	y = 782.16x + 6.07	0.999
62	Theaspirane	036431-72-8	28.62	1518	B		*y = 2034x	
63	3-Nonen-2-one	014309-57-0	28.81	1523	B		*y = 2034x	
64	Ethyl 3-hydroxybutanoate	005405-41-4	29.09	1530	B	Ethyl butanoate	y = 752.83x + 4.12	0.994
65	Benzaldehyde	000100-52-7	29.33	1536	A	Benzaldehyde	y = 185.13x + 2.44	0.998
66	Linalool	000078-70-6	30.10	1554	A	Linalool	y = 116.41x + 5.26	0.994
67	Ethyl 2-octenoate	002351-90-8	30.45	1563	B	Ethyl octanoate	y = 3657.96x + 1.74	0.997
68	1-Octanol	000111-87-5	30.62	1567	B		*y = 2034x	

(Continued on next page)

Supplemental Table 1. (*Continued*)

No.	Volatiles	CAS	RT[z]	RI[y]	Identification[x]	Quantitative standards	Standard curves[w]	R^2
69	2R,3S-Butanediol	000513-85-9	31.37	1585	A	2R,3S-Butanediol	y = 1526658.54x − 562.11	0.994
70	2,5-Dimethyl-4-methoxy −3(2H)-furanone	004077-47-8	32.17	1605	A	2,5-Dimethyl-4-methoxy −3(2H)-furanone	y = 4759.81x + 0.22	0.975
71	Hotrienol	029957-43-5	32.61	1617	B	Linalool	y = 116.41x + 5.26	0.994
72	Methyl benzoate	000093-58-3	33.33	1636	B		*y = 2034x	
73	β-Cyclocitral	000432-25-7	33.39	1637	B	Citral	y = 2933.16x − 4.83	0.998
74	Ethyl decanoate	000110-38-3	33.74	1646	A	Ethyl decanoate	y = 6319.51x + 64.86	0.995
75	Benzeneacetaldehyde	000122-78-1	34.01	1654	A	Benzeneacetaldehyde	y = 1232.06x + 8.69	0.999
76	Acetophenone	000098-86-2	34.46	1665	B	Benzeneacetaldehyde	y = 1232.06x + 8.69	0.999
77	1-Nonanol	000143-08-8	34.64	1670	B		*y = 2034x	
78	Ethyl (E)-4-decenoate	076649-16-6	34.84	1675	B	Ethyl decanoate	y = 6319.51x + 64.86	0.995
79	Ethyl benzoate	000093-89-0	35.05	1681	B		*y = 2034x	
80	α-Terpineol	000098-55-5	36.21	1709	A	α-Terpineol	y = 124.06x + 5.92	0.971
81	4-Ethyl benzaldehyde	004748-78-1	36.67	1724	B	Benzaldehyde	y = 185.13x + 2.44	0.998
82	Naphthalene	000091-20-3	37.94	1757	B	p-Cymene	y = 4174.67x + 4.91	0.997
83	Ethyl phenylacetate	000101-97-3	39.45	1797	A	Ethyl phenylacetate	y = 125.09 – 1.43	0.991
84	Nerol	000106-25-2	39.93	1811	A	Nerol	y = 828.26x + 2.12	0.962
85	3,4-Dimethyl benzaldehyde	005973-71-7	40.54	1828	B	Benzaldehyde	y = 185.13x + 2.44	0.998
86	Phenethyl acetate	000103-45-7	40.56	1829	A	Phenethyl acetate	y = 148.55x + 3.03	0.998
87	(E)-β-Damascenone	023726-93-4	40.88	1838	A	(E)-β-Damascenone	y = 82.21x + 5.93	0.997
88	1-(2,4-Dimethylphenyl)-ethanone	000089-74-7	41.20	1847	B	Benzeneacetaldehyde	y = 1232.06x + 8.69	0.999
89	(E,Z)-2,4-decadienoate	003025-30-7	41.39	1853	B	Ethyl decanoate	y = 6319.51x + 64.86	0.995
90	Hexanoic acid	000142-62-1	41.56	1858	A	Hexanoic acid	y = 111386.42x − 30.66	0.980
91	Benzyl alcohol	000100-51-6	42.71	1891	A	Benzyl alcohol	y = 2884.11x + 7.31	0.997
92	Phenylethyl alcohol	000060-12-8	43.98	1928	A	Phenylethyl alcohol	y = 2578.25x − 5.13	0.985
93	β-Ionone	000079-77-6	45.00	1957	B	α-Ionone	y = 130.01x + 10.71	0.997
94	Thymol	000089-83-8	53.41	2198	B		*y = 2034x	
95	Methyl anthranilate	000134-20-3	54.52	2230	A	Methyl anthranilate	y = 2162.59x + 9.63	0.992

[z]Retention times (RTs) were detected in the DB-WAX column.

[y]Retention indices (RIs) were calculated using DB-WAX column.

[x]Identification of volatiles: A, mass spectrum and RI agreed with standards; B, mass spectrum and RI agreed with NIST 2014 MS database and literature data.

[w]In standard curves, "y" indicates the concentration of volatiles (μg/L) and "x" indicates the area ratio of volatiles to internal standard (4-methyl-2-pentanol).

*Concentrations of these volatiles were expressed as the relative amount compared to the internal standard.

Supplemental Table 2. Total concentrations of isoprenoid-derived, fatty acid-derived, amino acid-derived, and other volatile in Shuijing grape berries during development [4–15 weeks after flowering (WAF)] in 2018 and 2019.

WAF	4	5	6	7	8	9	10	11	12	13	14	15
Isoprenoid-derived volatiles												
18RS			9.31 ± 0.05	9.78 ± 0.10	7.45 ± 0.03	8.55 ± 0.18	8.04 ± 0.03	9.27 ± 0.28	11.72 ± 0.30	15.03 ± 0.33	16.01 ± 0.86	25.29 ± 1.47
18OF	4.17 ± 0.09	7.89 ± 0.29	9.72 ± 0.13	9.79 ± 0.33	7.98 ± 0.17	11.43 ± 0.35	9.70 ± 0.21	8.87 ± 0.37	11.57 ± 0.33	13.13 ± 0.40	19.58 ± 0.38	27.15 ± 1.41
19RS			10.06 ± 0.49	12.79 ± 1.36	9.36 ± 0.82	8.89 ± 0.69	17.39 ± 0.83	18.22 ± 0.49	22.27 ± 1.46	27.99 ± 0.77	31.42 ± 2.10	29.14 ± 1.51
19OF	7.29 ± 0.46	10.68 ± 1.38	8.66 ± 0.41	11.63 ± 1.31	10.37 ± 0.67	8.87 ± 0.06	18.14 ± 3.21	20.66 ± 1.46	35.86 ± 0.80	44.30 ± 1.22	40.28 ± 4.80	30.97 ± 1.41
Fatty acid-derived volatiles												
18RS			275.20 ± 10.62	298.29 ± 8.87	318.44 ± 1.72	209.07 ± 14.29	172.79 ± 3.00	530.08 ± 32.80	1986.97 ± 15.26	3731.56 ± 43.63	4906.67 ± 60.48	9746.38 ± 854.56
18OF	216.80 ± 3.99	316.87 ± 2.20	325.40 ± 5.60	357.18 ± 7.53	353.96 ± 13.44	217.88 ± 6.15	161.43 ± 4.52	418.38 ± 22.36	2460.71 ± 36.80	4266.74 ± 17.08	8549.34 ± 90.23	14276.76 ± 383.30
19RS			861.62 ± 119.55	766.72 ± 146.02	462.83 ± 14.23	875.17 ± 92.29	1994.27 ± 334.03	3386.62 ± 151.18	4783.34 ± 220.13	6664.13 ± 88.62	8285.11 ± 663.99	11497.39 ± 517.60
19OF	357.50 ± 15.62	706.39 ± 47.14	404.74 ± 40.12	554.59 ± 49.41	519.49 ± 21.50	700.09 ± 71.98	1528.90 ± 145.58	3295.59 ± 101.56	5168.50 ± 242.05	7973.77 ± 245.11	10246.40 ± 975.18	14511.77 ± 1188.32
Amino acid-derived volatiles												
18RS			74.73 ± 2.11	101.33 ± 2.95	104.30 ± 1.82	106.72 ± 8.32	127.33 ± 2.29	144.76 ± 6.12	266.63 ± 9.62	896.08 ± 49.25	1306.16 ± 43.42	2464.80 ± 269.47
18OF	64.43 ± 1.18	67.41 ± 2.00	81.63 ± 1.30	112.93 ± 1.14	99.60 ± 1.04	107.09 ± 1.07	125.86 ± 2.79	154.06 ± 8.41	400.24 ± 3.67	925.21 ± 12.05	1749.50 ± 70.40	2506.80 ± 10.44
19RS			288.45 ± 8.14	422.01 ± 117.69	322.47 ± 9.65	379.81 ± 18.51	490.23 ± 64.42	916.61 ± 188.40	1957.79 ± 52.43	3180.11 ± 89.41	4405.16 ± 1174.80	4884.32 ± 1177.75
19OF	219.42 ± 131.33	206.78 ± 7.45	210.42 ± 40.40	307.17 ± 18.65	335.12 ± 8.22	348.89 ± 11.89	561.29 ± 145.49	978.59 ± 0.10	1798.78 ± 109.38	3127.28 ± 84.04	4273.48 ± 396.02	5147.59 ± 572.67
Other volatiles												
18RS			41.12 ± 4.54	66.32 ± 4.25	46.16 ± 2.31	27.98 ± 9.00	40.18 ± 1.75	29.96 ± 5.14	17.53 ± 2.36	10.93 ± 0.46	42.43 ± 1.86	212.20 ± 35.53
18OF	16.35 ± 1.05	79.87 ± 7.07	58.06 ± 6.45	58.27 ± 3.18	39.21 ± 3.20	35.65 ± 3.83	47.08 ± 3.51	35.14 ± 8.37	18.88 ± 2.05	9.27 ± 0.23	91.05 ± 1.92	483.11 ± 4.37
19RS			47.61 ± 3.77	46.96 ± 16.72	24.39 ± 1.61	26.02 ± 4.87	13.72 ± 0.70	25.45 ± 0.85	115.93 ± 3.92	270.07 ± 6.30	411.31 ± 75.55	863.87 ± 33.93
19OF	78.89 ± 16.50	67.34 ± 12.34	35.34 ± 6.98	46.48 ± 12.77	60.41 ± 6.38	41.09 ± 4.80	56.51 ± 12.39	23.52 ± 1.45	104.23 ± 4.55	227.71 ± 7.42	631.00 ± 108.59	1159.02 ± 20.07

OF = open field; RS = rain shelter.